Finite Element Method Based Elastic-Plastic Contact Behaviour of a Sphere Against a Rigid Flat – Effect of Strain Hardening

Ashok Kumar[1], Umasankar Das[2]

[1] Professor, Department of Mechanical Engineering, Raajdhani Engineering College Bhubaneswar, Odisha

[2]Associate. Professor, Department of Mechanical Engineering, Raajdhani Engineering College Bhubaneswar, Odisha

Abstract— The current study uses the finite element approach to analyze the elastic-plastic contact between a deformable sphere and a stiff flat. Using the commercial finite element program ANSYS, it is possible to examine the impact of strain hardening on the contact behavior of a non-adhesive frictionless elastic-plastic contact. We have used several tangent modulus values to study the strain hardening impact. Because the effect of strain hardening varied in how it affected the contact parameters, the resultant data clearly demonstrates that a generalized approach cannot be applied to all types of materials. This effect likewise gets stronger if the hardness parameter value gets bigger. The influence of strain hardening on contact characteristics is severe at higher values of the hardening parameter. The resistance of a material to deformation increases with strain hardening, and the material is able to carry a higher load in a smaller contact area

DOI Number: 10.48047/NQ.2021.19.8.NQ21157 **NeuroQuantology 2021;19(8):396-402**

.

I. INTRODUCTION

Surface interactions are dependent on the contacting materials and the shape of the surface. The shape of the surface of an engineering material is a function of both its production process and the nature of the parent material. When studied carefully on a very fine scale, all solid surfaces are found to be rough. So when two such surfaces are pressed together under loading only the peaks or the asperities of the surface are in contact and the real area of contact is only a fraction of the apparent area of contact. In such conditions the pressure in those contact spots are extremely high. Accurate calculation of contact area and contact load are of immense importance in the field of tribology and leads to an improved understanding of friction, wear, and thermal and electrical conductance between surfaces. But it is a difficult task as rough surfaces consist of asperities having different radius and height. The problem is simplified when Hertz [1] provides the contact analysis of two elastic solids with geometries defined by quadratic surfaces. From then the assumption of surfaces having asperities of spherical shape is adopted to simplify the contact problems and the elastic plastic contact of a sphere and flat becomes a fundamental problem in contact mechanics. Greenwood and Williamson [2] used the Hertz theory and proposed an asperity based elastic model where asperity heights follow a Gaussian distribution. The first plastic model was introduced by Abbott and Firestone [3] which neglects volume conservation of the plastically deformed sphere. The first model of elasto-plastic contact was proposed by Chang et al. [4]. In CEB model the sphere remains in elastic contact until a critical interference is reached, above which the volume conservation of the sphere tip is imposed. The CEB model suffers from a discontinuity in the contact load as well as in the first derivative of both the contact load and the contact area at the transition from elastic to elastic-plastic region. Later Evseev [5], Chang [6] and Zhao et al. [7] have made attempt to improve the elasto-plastic contact model.

Kogut and Etsion [8] (KE Model) first provide an accurate result of elastio-plastic contact of a hemisphere and a rigid flat. Kogut and Etsion used a finite element method to study the evaluation of the plastic zone in elastic-plastic contact between a sphere and rigid flat under frictionless contact condition. They study it for a wide range of material properties and sphere size and provide generalized empirical relations for contact area and contact force in terms of dimensionless contact interference for elastic, elastic-plastic and fully plastic region. They also studied their model for tangent modulus up to 0.1E and found negligible effect of it's in the contact parameters. Similar analysis has been done by Jackson and Green [9] (JG Model). In JG model they incorporated variation of material property (e.g. Hardness) on deformed geometry and presented some empirical relations of contact area and contact load. Kogut and Etsion [10] developed a statistical contact model based on the results of KE model [8]. Jackson and Green [11] have also done similar research. Quicksall et al. [12] used finite element technique to model the elasto-plastic deformation of a hemisphere in contact with a rigid flat for various materials such as aluminium, bronze, copper, titanium and malleable cast iron. They also studied the contact parameters for a generic material in which the elastic modulus and poisson's ratio were independently varied with the yield strength held constant and all the results are compared with the results of KE and JG Model. Brizmer et al. [13] have done elastic-plastic contact analysis between a sphere and rigid flat under perfect slip and full stick conditions for a wide range of material properties using FEM. According to the literature review contact analysis

*e*ISSN 1303-5150

of a deformable sphere with a rigid flat using FEM has done by several researchers and some of these studies consider the effect of material properties. But the effect of strain hardening on contact of deformable sphere and rigid flat in a detailed way is still missing. The present work aims to study the effect of strain hardening for single asperity contact for different values of hardening parameter which is related to the tangent modulus.

FINITE ELEMENT FORMULATION

The contact of a deformable hemisphere and a rigid flat is shown in Fig. 1 where the dashed and solid lines represent the

situation before and after contact respectively of the sphere of radius R. The figure also shows the interference (ω) and contact radius (a) corresponding to a contact load (P). The contact of deformable sphere with a rigid flat is modeled using finite element software ANSYS 10.0. Due to the advantage of simulation of axi-symmetric problems the model is reduced to a quarter circle with a straight line at its top.

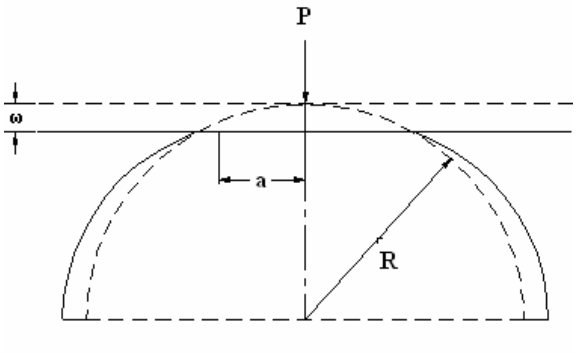

Fig. 1. A deformable sphere pressed by a rigid flat.

The quarter circle is divided into two different zone, e.g., zone I and zone II. Here zone I is within 0.1R distance from the sphere tip and zone II is the remaining region of the circle outside zone I. these two zones are significant according to their mesh density. The mesh density of zone I is high enough for the accurate calculation of the contact area of the sphere under deformation. Zone II has a coarser mesh as this zone is far away from the contact zone. The meshed model is shown in Fig. 2. The resulting mesh consists of 12986 no of PLANE82 and 112 no of CONTA172 elements. Here the arc of the circle represents the deformable contact surface and the straight line is the rigid flat.

The nodes lying on the axis of symmetry of the hemisphere are restricted to move in the radial direction. Also the nodes in the bottom of the hemisphere are restricted in the in the axial direction due to symmetry. The sphere size is used for this analysis is R = 0.01 mt. the material properties used here are Young's Modulus (E) = 70 GPa, Poission's Ratio (ν) = 0.3 and Yeild stress (σ_y) = 100 MPa. Here a frictionless rigid-deformable contact analysis is performed. In this analysis a bilinear material property, as shown in Fig. 3, is provided for the deformable hemisphere. To study the strain hardening effect we have taken different values of tangent modulus (E_t).The Tangent Modulus (E_t) is varied according to a parameter which is known as Hardening parameter and defined as, $H = \frac{E_t}{E - E_t}$. The value of H is taken in the range $0 \le H \le 0.5$ as most of the practical materials falls in this range. The value of H equals to zero indicates elastic perfectly plastic material (E_t =0) behavior which is an idealized material behavior. The hardening parameters used for this analysis and their corresponding values are shown in Table 1.

*e*ISSN 1303-5150

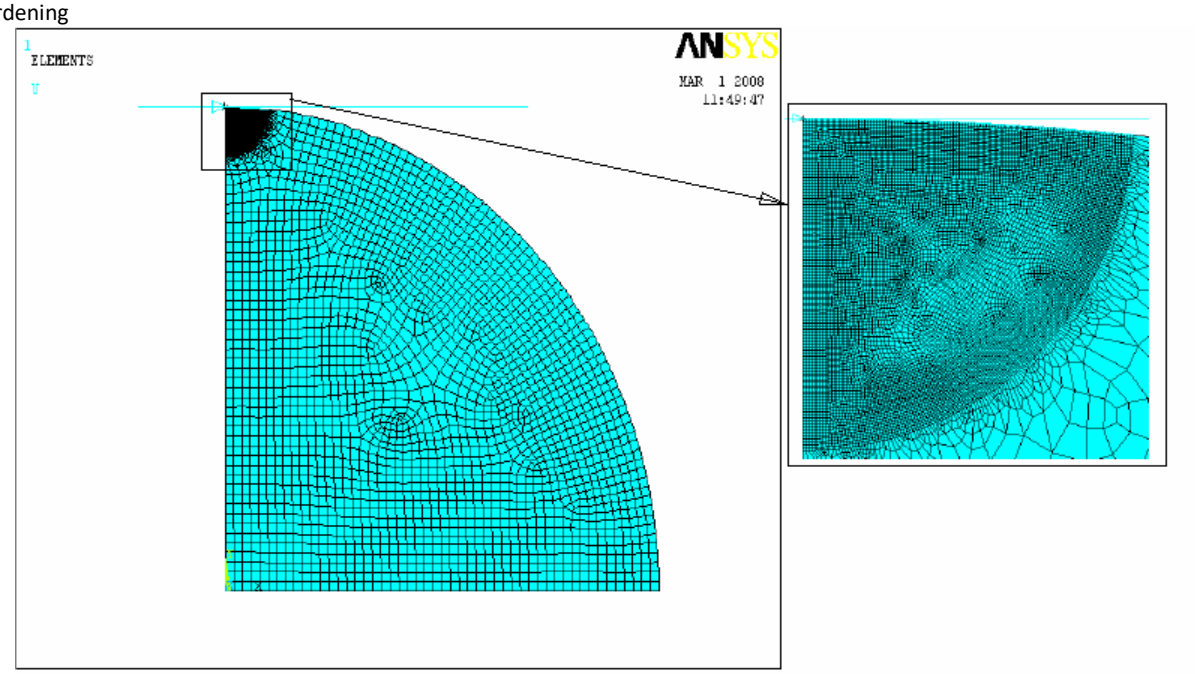

Fig. 2. Meshed model of the hemispherical contact

*e*ISSN 1303-5150

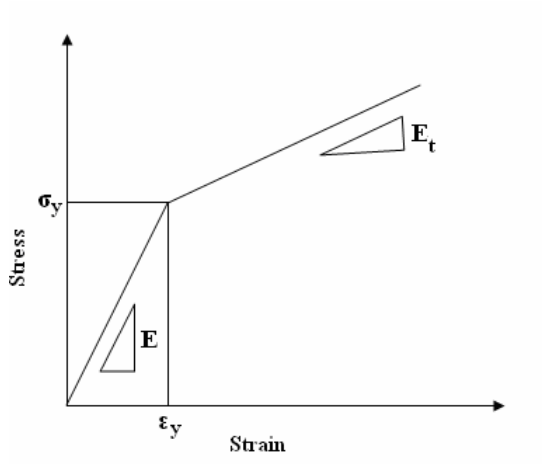

Fig. 3. Stress-strain diagram for a material having bilinear isotropic properties

TABLE 1

DIFFERENT H AND E_T VALUES USED FOR THE STUDY OF STRAIN HARDENING EFFECT

H	E_t in %E	E_t (GPa)
0	0.0	0.0
0.1	9.0	6.3
0.2	16.7	11.7
0.3	23.0	16.1
0.4	28.6	20.0
0.5	33.0	23.1

The wide range of values of tangent modulus is taken to make a fair idea of the effect of strain hardening effect in single asperity contact analysis. The solution type is chosen as large deformation static analysis. Here we have applied displacement on the target surface and the force on the hemisphere is found from the reaction solution. As this is an axi-symmetric analysis the force is calculated on a full scale basis. The radius of contact area is found from the last activated node for a particular analysis. In our analysis we have validated our mesh configuration by iteratively increasing the mesh density. The mesh density is increased by 1% until the contact force and contact area is differed by less than 1% between the iterations. In addition to the mesh convergence the model also compared with the Hertz elastic solution. The results of contact load are differed by maximum 3% and contact radius by not more than 5% below the critical interference.

II. RESULTS AND DISCUSSION

As discussed earlier the strain hardening effect is studied by varying the hardening parameter which in turn changes the value of tangent modulus while other material properties are kept constant. The model is validated by comparing the results for elastic perfectly plastic material condition, i.e. for $H = 0$, with the results of KE model [8]. The results are normalized according to the following normalization scheme. Interference is normalized by the critical interference, provided by Chang et al. [4]. The critical interference is defined as,

$$\omega_c = \left(\frac{\pi KS}{2E^*}\right)^2 R$$

Where, K is the hardness coefficient [$K = 0.454 + 0.41\nu$], S is the hardness of the material, according to Tabor [14] S is related to yield strength by $S = 2.8\sigma_y$ and E^* is the equivalent young's Modulus, $E^* = E/(1-\nu^2)$ in this case [E is the young modulus and ν is the Poisson's ratio of the deformable body]. The contact load is normalized according to critical contact load, i.e., load corresponding to critical interference and written as,

$$P_c = \frac{4}{3} E^* R^{1/2} \omega_c^{3/2}$$

The contact area is normalized according to critical contact area, i.e., area corresponding to critical interference and written as,

$$A_c = \pi R \omega_c$$

The results for elastic perfectly plastic material behavior are compared with the results of Kogut and Etsion. The calculated contact areas are exactly matched in the elastic and certain portion of the elastic plastic region and we found a maximum of 1% difference with the results KE model. In case of load vs. displacement we found there is a maximum of 3% difference with the results of KE model. Figs. 4 and 5 show the comparison of the load-interference and contact area-interference for the present case and the KE model.

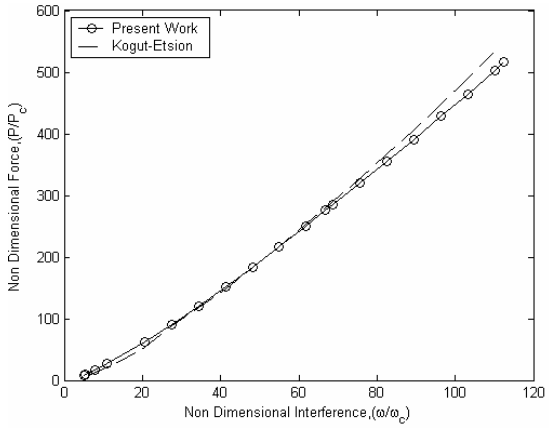

Fig. 4. Plot of contact load vs. interference for elastic perfectly plastic material

*e*ISSN 1303-5150

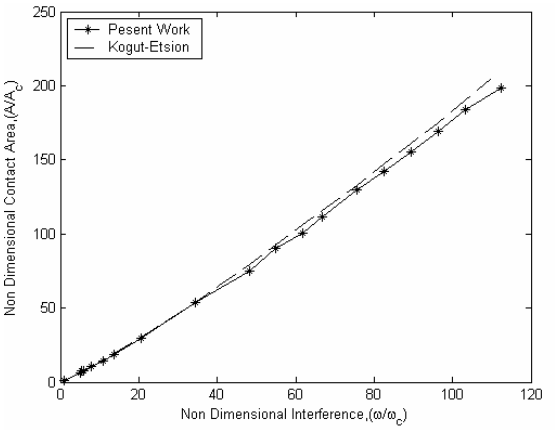

Fig. 5. Plot of contact area vs. interference for elastic perfectly plastic material.

The possible reason of this differences in the results is may be due to the fact that Kogut and Etsion have done this analysis for a large no of sphere radius in the range of $\leq R \leq 10$ (mm.) as well as for a large no of material properties in the range $100 \leq (E/\sigma_y) \leq 1000$ and they also found differences in their results up to 3%. Among all those results they provided the generalized one. Here we are representing the different contact conditions at different interference by means of stress contours of the deformed asperity. We found slightly higher values of interferences for the initiation of plastic and fully plastic deformation and as the differences are marginal, can be neglected. Von mises yield criterion is used to find the initiation of plastic deformation and fully plastic region is found when the mean pressure reaches the hardness value. The contour plots of von mises stress for different interference values are shown in Fig. 6.

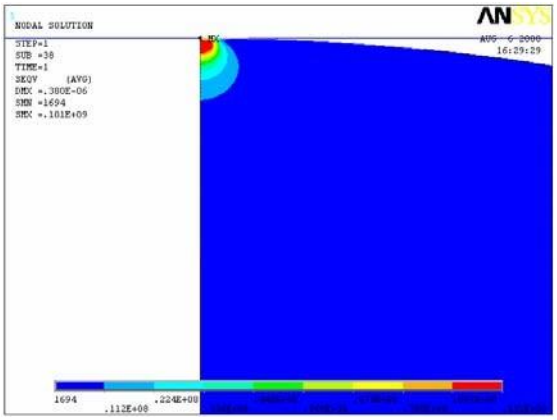

(a)

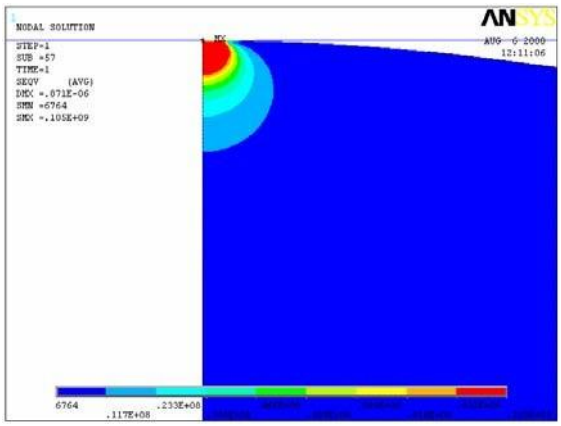

(b)

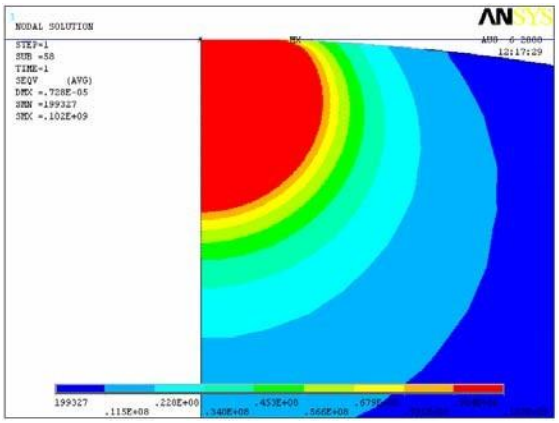

(c)

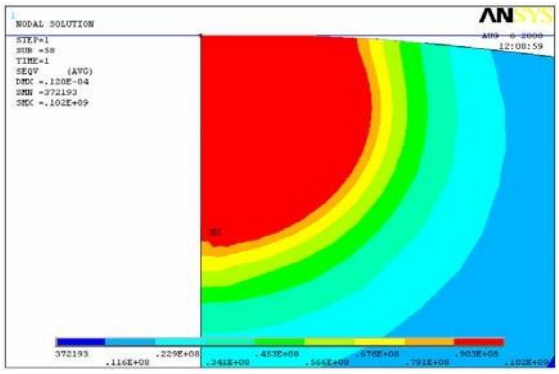

(d)

Fig. 6. Plot of von-mises stress for (a) ω = ωc, (b) ω = 6ωc, (c) ω = 68ωc and (d) ω = 110ωc

The effect of strain hardening effect in single asperity contact is studied for materials having different values of tangent modulus with the other material properties are taken as constant. Here we have studied it for an applied interference range of $10\omega_c \leq \omega \leq 200\omega_c$. Fig. 7 shows the

*e*ISSN 1303-5150

variation of contact load at different interference for materials having different values of tangent modulus. The plot shows a non linear behavior in between the load and interference as the results are in the elasto-plastic and fully plastic region. Similar non linear behavior is found in between contact area and interference which is shown in Fig. 8. These plots show that up to a certain value of non-dimensional interference $(\omega/\omega_c = 10)$ the effect of strain hardening on contact parameters become negligible. Here we found below this value the variations of results are in the range of 2-5% from that of elastic perfectly plastic material behavior. But a significant effect of strain hardening on contact parameters for higher interference values is found. It is also found that a small amount of stain hardening (with in 2% of E) helps in convergence of the solution and the results are quite close to the results of elastic perfectly plastic case. The variation of hardening parameters shows that for a small hardening parameter $H = 0.1$ the results of load and contact area varies 3-15% and 5-17% respectively from the results of elastic perfectly plastic case with in the elasto-plastic region, i.e. $10\omega_c \le \omega \le 110\omega_c$. For fully plastic region, i.e., $\omega > \omega_c$ these variations are quite high and increase monotonically with the increase in interference. While for the large hardening parameter $H = 0.5$ the variation in load and area are in the range of 11-52% and 5-33% respectively from that of elastic perfectly plastic case in the elasto-plastic region. In fully plastic region these variations are significantly high and increase monotonically with the increase in interference.

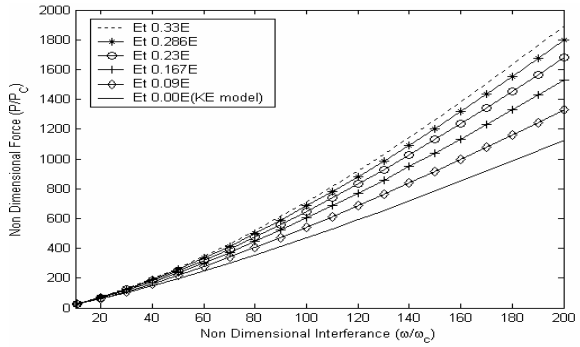

Fig. 7. Plot of contact load vs. interference for materials having various E_t values.

Fig. 7 also shows that with the increase in tangent modulus value the contact load increases at a particular interference value. This clearly indicates that the resistance to deformation of a material increases with the increase in tangent modulus value. Fig. 9 shows the variation of contact area at different applied load for materials having different values of tangent modulus. The figure shows a non linear behavior in between contact area and contact force. Here it is observed that the contact area decrease at a particular load for a material having higher tangent modulus value than that of a material having lower one. This indicates that with the increase in the effect of strain hardening the material can support the same applied load in a smaller contact area.

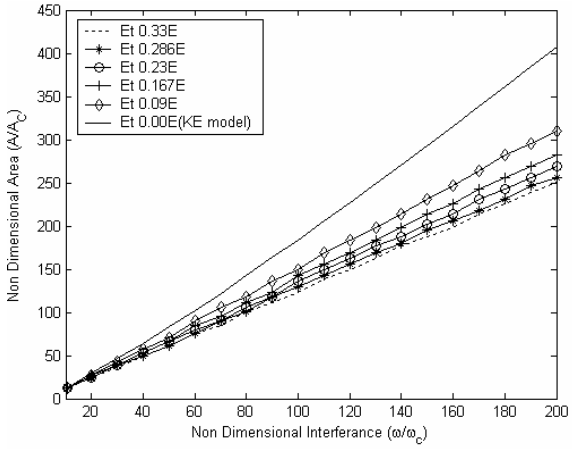

Fig. 8. Plot of contact area vs. interference for materials having different E_t values.

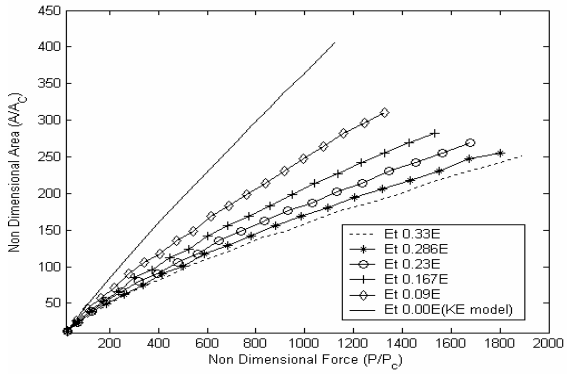

Fig. 9. Plot of contact area vs. force for materials having different E_t values.

III. CONCLUSIONS

The result of strain hardening effect clearly shows that a generalized solution can not be applicable for all kind of materials as the effect of strain hardening greatly influenced the contact parameters. With the increase in the value of hardening parameter this effect also increases. Thus for a particular material this parameter should be taken care appropriately to get the accurate prediction of contact load and contact area. It is also observed that a small amount of strain hardening improves the solution convergence. It is noticed that in the elasto-plastic region up to a certain interference value ($\omega = 10_c$) strain hardening have negligible effect on the contact parameters. If we assume that the material has very low hardening parameter, i.e. $H \le 0.1$, the effect of its quite small and can be neglected with marginal error in the elasto-plastic region but a significant effect of its is found in fully plastic region that can not be neglected. For higher value of hardening parameter the effect of strain hardening is severe on contact parameters. With the increase in strain hardening the resistance to deformation of a material is increased and the material becomes capable of carrying higher amount of load in a smaller contact area.

*e*ISSN 1303-5150

REFERENCES

[1] H. Hertz, "Über die Berührung fester elastischer Köper", *J. Reine and Angewandte Mathematik*, vol. 92, pp. 156-171, 1882.

[2] J. A. Greenwood, and J. B. P. Williamson, "Contact of nominally flat surfaces", *Proc. Roy. Soc. London A*, vol. 295, pp. 300-319, 1966.

[3] E. J. Abbott, and F. A. Firestone, "Specifying surface quality - a method based on accurate measurement and comparison", *ASME J. Mech. Engg*., vol. 55, pp. 569-572, 1933.

[4] W. R. Chang, I. Etsion, and D. B. Bogy, "An elastic-plastic model for the contact of rough surfaces", *ASME J. Tribol*., vol. 109, pp. 257-263, 1987.

[5] D. G. Evseev, B. M. Medvedev, and G. G. Grigoriyan, "Modification of the elastic-plastic model for the contact of rough surfaces", *Wear*, vol. 150, pp. 79-88, 1991.

[6] W. R. Chang, "An elastic-plastic contact model for a rough surface with an ion-plated soft metallic coating", *Wear*, vol. 212, pp. 229–237, 1997.

[7] Y. Zhao, D. M. Maietta, and L. Chang, "An asperity micro-contact model incorporating the transition from elastic deformation to fully plastic flow", *ASME J. Tribol*., vol. 122, pp. 86–93, 2000.

[8] L. Kogut, and I. Etsion, "Elastic-plastic contact analysis of a sphere and a rigid flat", *ASME J. Appl. Mech*., vol. 69, pp. 657–662, 2002.

[9] R. L. Jackson, and I. Green, "A finite element study of elasto-plastic hemispherical contact against a rigid flat", *ASME J. Tribol*., vol. 127, pp. 343-354, 2005.

[10] L. Kogut, and I. Etsion, "A finite element based elastic-plastic model for the contact of rough surfaces", *ASME J. Tribol*., vol. 46, pp. 383– 390, 2003.

[11] R. L. Jackson, and I. Green, "A statistical model of elasto-plastic asperity contact of rough surfaces", *Tribol. International*, vol. 39, pp. 906-614, 2006.

[12] J. J. Quicksall, R. L. Jackson, and I. Green, "Elasto-plastic hemispherical contact models for various mechanical properties", *Proc. Instn. Mech. Engrs., Part J: J. Engg. Tribol*., vol. 218, pp. 313–322, 2004.

[13] V. Brizmer, Y. Kligerman, and I. Etsion, "The effect of contact conditions and material properties on the elasticity terminus of a spherical contact", *Int. J. Solids Struct*., vol. 43, pp. 5736-5749, 2006.

[14] D. Tabor, *The Hardness of Metals*, Clarendon Press, Oxford, 1951.

*e*ISSN 1303-5150